Dark solitons in discrete lattices

Yuri S. Kivshar
Optical Science Centre, Research School of Physical Sciences, Australian National University, Canberra, Australian Capital Territory 0200, Australia

Wiesław Królikowski
Laser Physics Centre, Research School of Physical Sciences, Australian National University, Canberra, Australian Capital Territory 0200, Australia

Oksana A. Chubykalo
Departamento di Física Teórica I, Universidad Complutense, E-28040 Madrid, Spain
(Received 4 March 1994)

We analyze the effect of discreteness on properties and propagation dynamics of dark solitons in the discrete nonlinear Schrödinger equation. We show that for small-amplitude nonlinear waves the lattice discreteness induces novel properties of dark solitons, e.g., such solitons may be transformed into brightlike dark solitons on a modulationally stable background. For large-amplitude dark solitons we demonstrate that discreteness effects may be understood as arising from an effective periodic potential to the soliton's coordinate similar to the Peierls-Nabarro (PN) periodic potential for (topological) kinks in the Frenkel-Kontorova model. We calculate the PN barrier (the height of the PN potential) to a dark soliton numerically and, in the case of strong interparticle coupling, also analytically, and discuss how the existence of the PN barrier may affect the mobility of dark solitons in a discrete lattice. In particular, we predict unexpected types of discreteness-induced instabilities for soliton-bearing models showing that, even being at a bottom of the PN potential well, the dark soliton is unstable and it always starts to move after a series of oscillations around the potential minimum. An intuitive picture for such a discreteness-induced nonlinear instability of dark solitons is presented, and the novelty of this phenomenon in comparison to bright solitons is emphasized.

PACS number(s): 03.40.Kf, 63.20.Pw, 46.10.+z, 42.65.−k

I. INTRODUCTION

Solitons, coherent excitations of nonlinear physical models, are usually analyzed as solutions of partial differential equations. However, models describing microscopic phenomena in solids are inherently discrete, with the lattice spacing between the atomic sites being a fundamental physical parameter. For these systems, discreteness effects may modify drastically the dynamics of localized nonlinear excitations even in the framework of the simplest models (see, e.g., Refs. [1–12]). Another way to get discreteness effects strongly involved is to consider a system of *weakly coupled* nonlinear elements, e.g., interaction of many ($N \gg 2$) optical fibers in a specially designed periodic array of nonlinear waveguides (see, e.g., Refs. [13,14]).

Recently, interest in localized excitations in strongly anharmonic lattices has been increased by the identification of a new kind of strongly localized mode which may exist in homogeneous (i.e., without impurities) nonlinear lattices [3]. These modes are the discrete analog of the envelope solitons, with the unique property that their width (i.e., spatial extension) is only a few lattice spacings. One of the important features of these strongly localized modes is the existence of the effective periodic potential which affects free propagation of the modes through the lattice. This periodic potential resembles the famous Peierls-Nabarro (PN) potential known in the context of dislocation theory [15]. The existence of the PN potential reflects the fact that translational invariance in the system is broken by discreteness, and the translational (Goldstone) mode no longer exists. From the physical point of view, the amplitude of the PN potential may be viewed as the minimum barrier which must be overcome to translate the dislocation by one lattice period. In the context of nonlinear localized modes in lattice models, the PN potential was discussed in several recent papers [6–8,10,12], and it was pointed out that the existence of the PN barrier may explain the stability properties of nonlinear modes: it seems that the stable mode always corresponds to an extrema of the PN potential [6,8,12].

An important question arises when one compares nonlinear modes in discrete lattices with those which may be found in the continuum limit approximation, e.g., that described by an effective (continuous) nonlinear Schrödinger (NLS) equation. As is known (see, e.g., Ref. [16]), spatially localized modes may be understood as a highly discrete version of the so-called *bright envelope solitons* of the continuous NLS equation which exist under the condition of modulational instability of the continuous wave (cw). However, it is known that when the cw solution is *modulationally stable*, nonlinear localized modes may exist on a stable cw background wave in the

form of *dark solitons*.

Interest in studying dark solitons has recently increased in connection with problems of nonlinear optics, where dark solitons were shown to create perfect self-induced optical waveguides to guide, steer, or switch one optical beam by another (see, e.g., [17,18] and also the recent review paper [19] and references therein). For a controllable soliton-based optical switching it is necessary to propose *multiport* nonlinear devices where more than two optical modes interact. Thus, *waveguide arrays* seem to be natural objects which may allow multiport beam coupling, steering, and switching. As was shown in Ref. [13], such arrays are described, in the main approximation, by the discrete NLS equation and, therefore, it is important to analyze how the soliton-based guiding and switching already observed in bulk materials [17] may be extended to be used for such discrete systems. This will be useful also to compare the properties of the soliton-based switching based on dark solitons with those already discussed for the case of bright solitons in waveguide arrays [20–22].

It is the main purpose of the present paper to analyze, within the framework of the discrete (nonintegrable) NLS equation, the effects of discreteness and the influence of the effective PN potential on propagation and properties of dark solitons in discrete models. In particular, we calculate the PN barrier (the height of the PN potential) to a dark soliton and show analytically and numerically *how* the lattice discreteness may affect the dark-soliton mobility.

The paper is organized as follows. In Sec. II we discuss our model, showing that a rather wide class of physical problems may be reduced to the discrete NLS equation, the main object of our analysis in this paper. It includes also a brief summary of (rather known) results of the quasicontinuum theory of nonlinear waves in lattices which may describe dark solitons using the so-called discrete-carrier-wave approximation. The main results of our analysis of the PN potential are presented in Secs. III and IV. Section III includes the calculation of the PN barrier for a dark soliton, numerically and analytically. In Sec. IV we discuss how the lattice discreteness may affect the dark-soliton mobility and we predict a novel type of discreteness-induced instability in soliton-bearing lattice models. Finally, Sec. V concludes the paper.

II. DISCRETE SOLITONS AND QUASICONTINUUM APPROXIMATION

A. Model

The main object of our analysis is the discrete (nonintegrable) version of the NLS equation, which we write in the form

$$i\frac{d\psi_n}{dt} + D(\psi_{n+1} + \psi_{n-1} - 2\psi_n) + \lambda|\psi_n|^2\psi_n = 0. \quad (1)$$

Equation (1) appears in nonlinear problems of very different physical origin. For example, it describes the self-trapping phenomenon in a variety of coupled-field theories where the discreteness effects are important, from the self-trapping of vibron modes in bimolecules (see, e.g., Ref. [23]) to the dynamics of linear arrays of vortices (see, e.g., Ref. [24]). Another application of the model (1) has been mentioned in the Introduction: The discrete NLS equation (1) describes the interaction of TE modes of the electromagnetic field in an array of nonlinear waveguides (see, e.g., Refs. [13,14,20–22]).

The discrete NLS equation (1) may be also derived in a one-frequency approximation from the standard (discrete) model a of one-dimensional chain of particles subjected to a nonlinear (on-site) substrate potential,

$$U(u_n) = \frac{m\omega_0^2}{2}u_n^2 + \frac{\alpha}{3}u_n^3 + \frac{\beta}{4}u_n^4, \quad (2)$$

where u_n is the displacement of the nth particle from the equilibrium position, m is the particle's mass, ω_0 is the frequency of small-amplitude (on-site) vibrations of a particle in the substrate potential, and α and β are the (cubic and quartic) anharmonicity parameters of the potential. Analyzing slow temporal variations of the wave envelope in such a chain and looking for solutions in the form

$$u_n = \phi_n + \psi_n e^{-i\omega_0 t} + \xi_n e^{-2i\omega_0 t} + \text{c.c.}, \quad (3)$$

where c.c. stands for complex conjugate, we finally obtain two algebraic relations for the functions ϕ_n and ξ_n,

$$\phi_n = -\frac{2\alpha}{\omega_0^2}|\psi_n|^2, \quad \xi_n = \frac{\alpha}{3\omega_0}\psi_n^2,$$

and the discrete NLS equation for the first harmonic ψ_n in the form (1) where the coefficients D and λ are expressed through the parameters of the linear and nonlinear interactions (see [25]),

$$D \equiv \frac{k_2}{2m\omega_0}, \quad \lambda \equiv \frac{1}{2m\omega_0}\left(\frac{10\alpha^2}{3\omega_0^2} - 3\beta\right), \quad (4)$$

and k_2 characterizes interaction of nearest neighbors in the lattice. The basic approximation used to derive the discrete NLS equation from the model of a discrete chain with the on-side potential (2) is the assumption $m\omega_0^2 \gg 4k_2$ which for lattices means that the linear spectrum band, which is proportional to $\sqrt{k_2/m}$, is rather narrow in comparison with the spectrum gap ω_0, i.e., discreteness effects are strong enough.

Equation (1) has an exact cw solution,

$$\psi_n(t) = \Psi_0 e^{i\Theta}, \quad \Theta = \tilde{q}na - \tilde{\omega}t, \quad (5)$$

where the frequency $\tilde{\omega}$ obeys the nonlinear dispersion relation, $\tilde{\omega} = 4D\sin^2(\tilde{q}a/2) - \lambda|\Psi_0|^2$. It is known (see, e.g., Ref. [5]) that the modulational instability of the cw solution (5) depends on the carrier wave number $\tilde{q}$ and the cw mode becomes unstable provided

$$\lambda\cos(\tilde{q}a) > 0. \quad (6)$$

The result (6) determines the condition for spatially localized modes to exist. However, if $\lambda\cos(\tilde{q}a) < 0$, the cw solution (8) is modulationally stable, and nonlinear localized modes may be expected to exist in the form of dark solitons.

B. Quasicontinuum approximation

The standard way to analyze bright and dark solitons in a lattice is to use the so-called discrete-carrier-wave approximation. This approach considers the cw background (carrier) wave as a solution of the lattice equations, but localized modes (e.g., dark solitons) are treated in the continuum approximation. In that case it is naturally assumed that the soliton's width is much larger than the lattice spacing, and the only way for the discreteness effects to come into the play is to renormalize the coefficients of the effective (continuous) NLS equation.

Following that idea we look for a solution of Eq. (1) in the form

$$\psi_n(t) = \Psi(n,t)\exp(iQan - i\Omega t), \tag{7}$$

where it is assumed that Q and Ω obey the linear dispersion relation, $\Omega = 4D\sin^2(Qa/2)$. Expanding the slowly varying envelopes $\Psi(n\pm1,t)$ into a Taylor series, we come to the continuous NLS equation

$$i\frac{\partial\Psi}{\partial t} + iV_g\frac{\partial\Psi}{\partial x} + \frac{1}{2}\Delta\frac{\partial\Psi}{\partial x^2} + \lambda|\Psi|^2\Psi = 0, \tag{8}$$

where

$$V_g \equiv \frac{d\Omega}{dQ} = 2aD\sin(Qa) \tag{9}$$

is the group velocity and the parameter Δ,

$$\Delta \equiv 2\frac{d^2\Omega}{dQ^2} = 2a^2D\cos(Qa), \tag{10}$$

describes the group-velocity dispersion of the waves. The condition (6) simply means that the nonlinearity and dispersion terms are of the same sign; this is the necessary condition for modulational instability described by the NLS-like models. In the case $\lambda\Delta < 0$, i.e., $\lambda\cos(Qa) < 0$, the continuous NLS equation (11) has an exact solution describing a dark soliton of an arbitrary amplitude. This means that, for $\lambda > 0$, dark solitons exist if $\cos(Qa) < 0$, i.e., for high-frequency oscillations, when adjacent particles move out of phase. But for $\lambda < 0$ low-frequency oscillations are modulationally stable, and dark-solitons are possible as hole excitations in the background oscillations when the adjacent particles move in phase.

For $\lambda = -|\lambda| < 0$ the dark-soliton solution of Eq. (8) has the well-known form

$$\Psi(x,t) = \Psi_0\left\{B\tanh Z + iA\right\}e^{-i|\lambda|\Psi_0^2 t}, \tag{11}$$

where

$$Z = \Psi_0 B\sqrt{|\lambda|/\Delta}(x - W\,t) \tag{12}$$

and

$$W = V_g + \Psi_0 A, \quad A^2 + B^2 = 1. \tag{13}$$

As a matter of fact, the parameter A characterizes the velocity of the dark soliton in the reference frame moving with the group velocity V_g. However, in two particular cases, $Q = 0$ and $Q = \pi$, the background wave is at rest [see Eq. (9)] and the parameter A describes the velocity of the dark soliton itself. The velocity of the dark soliton determines also its "contrast," i.e., a ratio of the minimum intensity of the soliton to the background (maximum) intensity. The simple relation

$$|\Psi|^2 = \Psi_0^2\left(1 - \frac{B^2}{\cosh^2 Z}\right), \tag{14}$$

where Z is defined in Eq. (12), shows that the parameter $B \equiv \sqrt{1-A^2}$ has a sense of the dark-soliton contrast; the dark solitons moving faster have smaller amplitude.

The results presented above are, generally speaking, similar to those already established for other lattice models supporting soliton propagation and, as a matter of fact, they do not take into account the effect of discreteness on the dark soliton. The lattice origin of the model (1) manifest itself in Eq. (8) only in the explicit expressions for the group velocity V_g and the group velocity dispersion Δ, and these parameters are mainly responsible for conditions for dark solitons to exist.

III. EFFECTS OF LATTICE DISCRETENESS

A. Small-amplitude ("gray") solitons

The simple way to analyze the effect of discreteness on the propagation dynamics and properties of dark solitons is to use the so-called small-amplitude limit. In the case of small amplitudes the solitons are rather wide [see Eqs. (11)–(13), where the small-amplitude limit corresponds to the condition $B^2 \ll 1$], and the discreteness effects may be analyzed by taking into account the next-order terms in the Taylor expansion,

$$i\frac{\partial\psi}{\partial t} + a^2D\frac{\partial^2\psi}{\partial x^2} + \frac{a^4D}{12}\frac{\partial^4\psi}{\partial x^4} - |\lambda||\psi|^2\psi = 0, \tag{15}$$

where $x = na$ is considered as a continuous variable. Looking for a solution of Eq. (15) in the form

$$\psi(x,t) = [\Psi_0 + a(x,t)]\exp\left\{-i|\lambda|\Psi_0^2 t + i\phi(x,t)\right\}, \tag{16}$$

and assuming that the condition of small amplitude is always fulfilled, $a \ll \Psi_0$, we may obtain a system of two coupled equations for the functions a and ϕ (see details in Ref. [26]). That system may be analyzed by applying the asymptotic expansion method, i.e., using the power-series expansions

$$a = \epsilon^2 a_0 + \epsilon^4 a_1 + \cdots, \quad \phi = \epsilon\phi_0 + \epsilon^3\phi_1 + \cdots, \tag{17}$$

and "slow" variables,

$$\tau = \epsilon^3 t, \quad z = \epsilon(x - Ct), \tag{18}$$

where ϵ is a small (scaling) parameter, and C is the phase velocity ("sound speed") of linear waves propagating on the background of the amplitude Ψ_0,

$$C^2 = 2|\lambda|a^2 D\Psi_0^2. \tag{19}$$

As a result, in the lowest order in the small parameter ϵ we obtain the well-known Korteweg–de Vries equation for the soliton amplitude a_0,

$$2C\frac{\partial a_0}{\partial \tau} + G_1 a_0 \frac{\partial a_0}{\partial z} - G_2 \frac{\partial^3 a_0}{\partial z^3} = 0, \tag{20}$$

where the variables z and τ are introduced above, the coefficients G_1 and G_2 are defined by the relations

$$G_1 = 12|\lambda|a^2 D\Psi_0, \quad G_2 = a^4 D\left(1 - \frac{|\lambda|\Psi_0^2}{6D}\right), \tag{21}$$

and the phase ϕ_0 is determined by the equation

$$\frac{\partial \phi_0}{\partial z} = \frac{4\Psi_0}{C} a_0. \tag{22}$$

Equation (20) has a soliton solution

$$a_0(z,\tau) = -(12\mu^2 G_2/G_1)\,\mathrm{sech}^2[\mu(z - W\tau)], \tag{23}$$

where $W = -2\mu^2 G_2/C$ is the soliton velocity in the reference frame moving with the sound speed C, and μ is an arbitrary parameter which defines the soliton amplitude.

The results presented above show how the parameters of a dark soliton in this (small-amplitude) limit are modified by discreteness. In particular, as clearly seen from Eqs. (21) and (23), increasing the amplitude of the cw background Ψ_0 causes the effects produced by discreteness more and more important because in this case the effective interaction between particles in the lattice (which is proportional to $D/|\lambda|\Psi_0^2$) becomes weaker. For

$$|\lambda|\Psi_0^2 > 6D \tag{24}$$

the soliton (23) may change the sign of its amplitude transforming into an antidark (or brightlike dark) soliton on a cw background. The transformation of a dark soliton into an antidark soliton due to higher-order (in fact, third-order) dispersion contribution was discussed in Ref. [27]. The possibility of existence of antidark solitons in the discrete NLS was observed numerically in Ref. [28]. However, the authors of Ref. [28] tried to analyze this phenomenon in the region of the parameters when the condition (24) is not fulfilled. Our numerical simulations of the dynamics of the discrete NLS equation with the soliton given by the formulas (16)–(18) and (21)–(23) as an initial condition shows that the antidark soliton is stable and its propagation does not lead to any sufficient radiation. In Fig. 1 we present the dynamics of such a soliton on the background $\Psi_0 = 2.0$ (not shown in the picture) for the standard choice of the lattice parameters, $D = 1.0$ and $a = 1.0$. Similar to the case of the third-order dispersion [27], the antidark soliton propagation looks radiationless and the soliton shape is preserved due to a balance of dispersion effects and nonlinearity, as is well known for dynamical solitons of the Korteweg–de Vries equation.

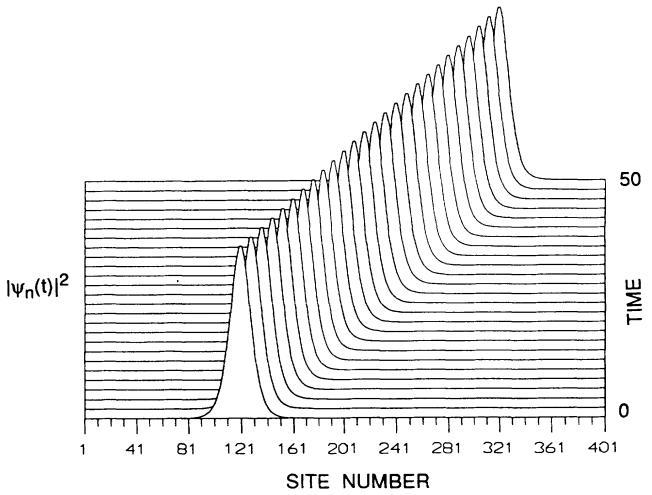

FIG. 1. Dynamics of an antidark pulse supported by the lattice discreteness. Initial conditions (16)–(23) at $\Psi_0 = 2.0$, $D = 1.0$, and $a = 1.0$.

Thus, even in the small-amplitude limit one observes that discreteness may drastically modify the properties of a dark soliton and, in particular, change the sign of the soliton's amplitude due to a contribution of higher-order dispersion effects.

B. Peierls-Nabarro barrier to a dark soliton

The importance of discreteness on the dark-soliton propagation in nonlinear lattices may be clearly seen when the velocity of the soliton relative to the background plane wave is small. This is the case of large-amplitude dark solitons, which have the intensity at the minimum close to zero. In the continuum approximation this solution is given by the simple analytical expression [cf. Eq. (14)]

$$\psi(x,t) = \Psi_0 \tanh\left[\Psi_0\sqrt{\frac{|\lambda|}{\Delta}}(x - x_0)\right] \exp\left\{-i|\lambda|\Psi_0^2 t\right\}. \tag{25}$$

Trying to use this solution as a continuum limit of a dark soliton on a lattice, one notes that the resulting particle configuration representing the solution (25) depends on the position of the soliton coordinate x_0. Thus, the solution (25) on a lattice presents a family of different dark-soliton solutions which are characterized by the parameter x_0 and not connected to each other by a simple translation. To analyze the effect of discreteness on the stationary dark-soliton mode, we look for the *stationary solution* of Eq. (1) in the form

$$\psi_n = \Psi_0 f_n \exp\left(-i|\lambda|\Psi_0^2 t\right), \tag{26}$$

where it is assumed that the real function f_n does not depend on time [cf. Eq. (25)]. Then, for the function f_n the following nonlinear difference equation holds:

$$K(f_{n+1} + f_{n-1} - 2f_n) = (f_n^2 - 1)f_n, \tag{27}$$

where

$$K \equiv \frac{D}{|\lambda|\Psi_0^2}. \tag{28}$$

Here we assume that $\lambda = -|\lambda| < 0$, i.e., the dark-soliton modes are considered to be excited on a background consisting of in-phase particle oscillations. As a matter of fact, the consideration presented below may be easily extended to cover the case of high-frequency oscillations when dark-soliton modes may exist on a background consisting of out-of-phase particle oscillations; this is valid for $\lambda > 0$. Indeed, we note that Eq. (1) allows the transformation

$$\psi_n(\lambda > 0) = (-1)^n \psi_n(\lambda < 0) e^{-4iDt}, \tag{29}$$

where $\psi_n(\lambda < 0)$ and $\psi_n(\lambda > 0)$ stand for solutions of Eq. (1) for $\lambda < 0$ and $\lambda > 0$, respectively. In this second case, looking for the stationary solution in the form

$$\psi_n(t) = (-1)^n \Psi_0 f_n \exp\left[-i(4D + \lambda\Psi_0^2)t\right], \tag{30}$$

we find that the function f_n satisfies again Eq. (27). Note, however, that the energies of low-frequency (E_-) and high-frequency (E_+) modes are connected by the simple relation

$$E_+ = 4KN - E_-, \tag{31}$$

where

$$N = \sum_n f_n^2, \tag{32}$$

and

$$E_- = \sum_{n=-\infty}^{\infty} \left\{ K(f_{n+1} - f_n)^2 + \frac{1}{2}(f_n^2 - 1)^2 \right\}. \tag{33}$$

To find the form of localized solutions of Eq. (27) describing the profile of a dark soliton on the lattice, we solve Eq. (27) assuming the boundary conditions similar to those of the continuum limit case [see Eq. (25)], i.e., $f_n^2 \to 1$ for $n > N$ (N is large enough), and also the symmetry condition, e.g., $f_n = -f_{-n}$. However, in the discrete case the center of such a solution may vary in the interval $0 < x_0 \leq a$, a being the lattice spacing. In the analogy to the case of bright solitons [6], we analyze two special cases of stationary solutions when the dark soliton is centered either at a particle site or between the nearest particle sites [see Figs. 2(a) and 2(b)]. Indeed, when moving along the chain, a dark-profile mode changes its position and, correspondingly, its structure. Thus, exactly as in the case of bright solitons, two stationary

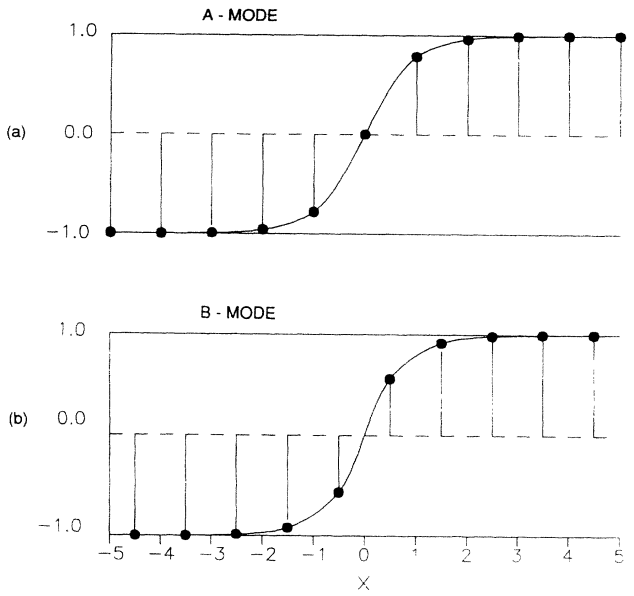

FIG. 2. Profiles of low-frequency ($\lambda < 0$) dark solitons in the lattice with $K = 0.5$, when the stationary mode is centered on a site (a) and between two neighboring sites (b). Note that in each case the background shows the in-phase oscillations of neighboring particles as one would expect for the acoustic modes.

modes shown in Figs. 2(a) and 2(b) (i.e., one centered at the particle site and the other one centered between the sites) may be viewed as those related by translations of 1/2 lattice spacing and, therefore, they both "occur" as two "states" of a single mode translating through the lattice. Our present study confirms that these two stationary modes can indeed be viewed as belonging to a single dark-profile mode and that the difference in their energies may be attributed to *the height of an effective periodic potential* generated by the lattice discreteness. This potential resembles the PN potential known in the context of dislocation theory [15]. As has been mentioned in the Introduction, the existence of the PN barrier reflects the fact that translational invariance is broken by discreteness, and the translational (Goldstone) mode no longer exists. From the physical point of view, the amplitude of the PN potential may be treated as the minimum barrier which must be overcome to translate the dislocation by one lattice period. In the context of nonlinear localized modes in lattice models, the PN potential has been recently discussed by Kivshar and Campbell [6] (see also Refs. [7,10,12]).

Analogously to the approach used in [6], we define two stationary configurations [see Figs. 2(a) and 2(b)]. In the first case, which we call the A mode [see Fig. 2(a)], the mode satisfies the conditions $f_0 = 0$ and $f_1 = -f_{-1}$. The corresponding energy in this case may be written as

$$E_A = \frac{1}{2} + 2\sum_{i=1}^{\infty} \left\{ K(f_{i+1} - f_i)^2 + \frac{1}{2}(f_i^2 - 1)^2 \right\}. \tag{34}$$

In the second case [the so-called B mode; see Fig. 2(b)] the mode is determined by the condition $f_1 = -f_0$ and it has the energy

$$E_B = K(2f_1)^2 + 2\sum_{i=1}^{\infty}\left\{K(f_{i+1}-f_i)^2 + \frac{1}{2}(f_i^2-1)^2\right\}. \tag{35}$$

Knowing the value of the two first displacements f_0 and f_1, we can find the displacement of the next particle from the relation Eq. (27). Therefore, using a simple iteration procedure for the only unknown value f_1 and applying the conditions $f_{n-1} < f_n$, we can find the unique value of f_1 leading to the localized dark-soliton solution on the lattice. The particular cases of dark-soliton profiles at $K = 0.5$ for low-frequency oscillatory background ($\lambda < 0$, in-phase oscillations) and high-frequency oscillatory background ($\lambda > 0$, out-of-phase oscillations) are shown in Figs. 2 and 3, respectively.

If the difference between the energies of the A and B modes is nonzero, the dark soliton cannot move freely through the lattice. It remains pinned, and the energy difference

$$\varepsilon_{PN} = |E_A - E_B| \tag{36}$$

has the sense of the pinning energy. The value (36) defines the amplitude of the PN barrier to the dark soliton. This value may be easily calculated numerically as a function of the coupling constant K (see Fig. 4).

It is not difficult to obtain an analytical estimation of the value (36) in two limiting cases: the quasicontinuum approximation ($K \gg 1$) and the highly discrete limit ($K \ll 1$). In the first case, to take into account discreteness of the lattice in a simple way, we present the dark-soliton solution in the form

$$f_n = \tanh[B(an - x_0)], \tag{37}$$

where $B = 1/\sqrt{2K}a \ll 1$. The discrete energy defined by Eq. (33) is a function of the position of the soliton center, x_0, and after simple transformations it may be written as

$$E = \sum_{n=-\infty}^{\infty} \frac{1}{\cosh^4[B(an - x_0)]}. \tag{38}$$

To calculate this quantity we use the well-known Poisson formula (see, e.g., Ref. [7]) to transform the sum into the integral

$$E = \int_{-\infty}^{\infty} \frac{(dx/a)}{\cosh^4[B(x - x_0)]}\left\{1 + 2\sum_{s=1}^{\infty}\cos\left(\frac{2\pi s x}{a}\right)\right\}. \tag{39}$$

In the case $B \gg 1$, we take into account only the most significant terms, thus arriving for large values of K at the expression

$$E \approx \frac{2\sqrt{2K}}{3}\left[1 + 8\sqrt{2}K^{\frac{3}{2}}\pi^4\exp(-\pi^2\sqrt{2K}) \times \cos\left(\frac{2\pi x_0}{a}\right)\right]. \tag{40}$$

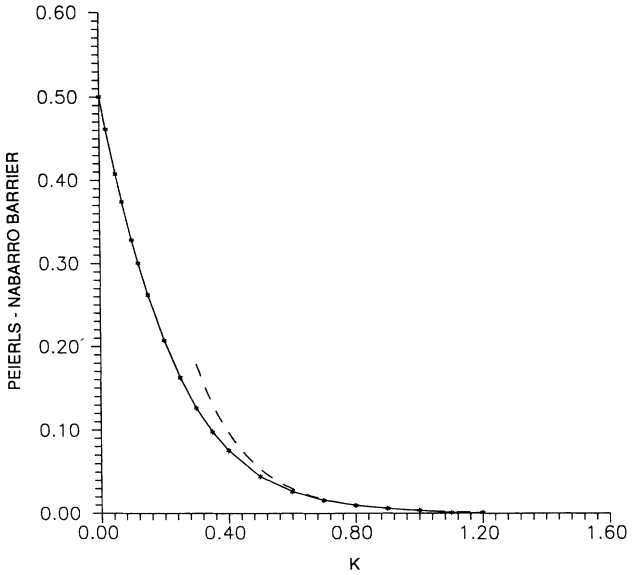

FIG. 4. The Peierls-Nabarro barrier to a dark soliton in the discrete NLS equation (1) as a function of the coupling parameter $K = D/|\lambda|\Psi_0^2$, which depends on the value of the background intensity. Solid line with stars: results of numerical calculations; dashed line: analytical results given by Eq. (41). Note that good agreement between analytical and numerical results may be already observed for $K \geq 0.5$.

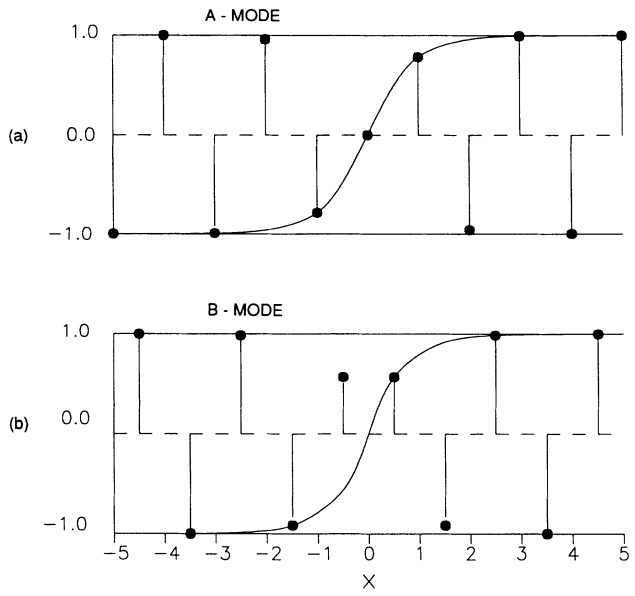

FIG. 3. Profiles of high-frequency ($\lambda > 0$) dark solitons in the lattice with $K = 0.5$, when the stationary mode is centered on a site (a) and between two sites (b). Note that in this case the background shows out-of-phase oscillations of neighboring particles corresponding to the structure of opticlike modes.

Therefore, in the framework of this "quasidiscrete approximation," the effective energy of the dark soliton is an oscillatory function of the soliton position x_0, and extremum points correspond to stationary configurations, i.e., $x_0 = 0$, to the A mode shown in Fig. 2(a), and $x_0 = a/2$, to the B mode shown in Fig. 2(b). From Eq. (40) we obtain the value of the PN potential barrier as

$$\varepsilon_{PN} = |E_A - E_B| = \frac{2^7\pi^4K^2}{3}\exp(-\pi^2\sqrt{2K}), \quad (41)$$

which is exponentially small for large values of K. The function (41) is shown in Fig. 4 by a dashed line. Note the very good agreement between numerical results and the analytical formula (41) even for $K \sim 1$. For instance, at K=1.0, from Eq. (41) we find $\varepsilon_{PN} \simeq 3.61\times10^{-3}$ while its exact numerical value is $\simeq 3.66 \times 10^{-3}$. In the limit $K \to 0$, the function $\varepsilon_{PN}(K)$ tends to a finite value which in dimensionless units equals 1/2. This result has very simple physical explanation: in the limit of weakly interacting particles the stationary structures given by the A and B modes [shown in Figs. 2(a) and 2(b), respectively] differ in the energy of a single-particle oscillation which, as follows from Eqs. (34) and (35), is just 1/2 in dimensionless units adopted in Eq. (27). Additionally, the PN barrier may be easily calculated analytically also for the case of weak coupling as an expansion in small K.

Finally, we would like to mention that the similar analysis is also valid for high-frequency dark-soliton modes. In fact, as has been mentioned before, all the configurations for stationary dark-profile modes are defined by the same functions through the relation (30). Additionally, the energies of high- and low-frequency modes are connected in a similar way, as may be seen from Eq. (31). A more detailed analysis of high-frequency modes and their discreteness-induced dynamics is presented below.

IV. HOW DOES A DARK SOLITON SENSE THE PN BARRIER ?

A. Simplest collective-coordinate analysis

1. Low-frequency modes

The stationary modes analyzed above correspond to extrema points of the effective PN potential. It is clear that such stationary points may be minima, maxima, or saddle points in the effective phase space of the discrete dynamical system (1). To analyze the stability properties of the localized modes in the vicinity of a stationary point, we should consider the full dynamical system (1). Because the model (1) is not integrable, such an analysis is rather difficult to carry out even in the limit of small oscillations around the stationary point and one of the possible ways is to use direct numerical simulations to the problem. Another way is to use the so-called *collective-coordinate approach*, introducing an effective ansatz to model the localized solution and treating its parameters as functions of time. This method is one of the versions of the so-called variational approach, with the main difference in the ansatz, which is in this case very close to the known exact localized solution of the problem in the continuum approximation. The variational approach is known to be *the simplest method* to describe general features of the nonlinear dynamics with particlelike excitations (see, e.g., Ref. [29] and references therein). At the same time, this is not a rigorous method, and for specific effects the results are rather sensitive to the successful choice of trial functions. The optimum is to combine such a variational approach with numerical calculations to obtain a rather realistic picture of the system dynamics.

First, we analyze the case of a dark soliton excited on a modulationally stable in-phase background oscillation. This case is realized for $\lambda = -|\lambda| < 0$. We start from the discrete NLS equation [cf. Eq. (1)]

$$i\frac{d\psi_n}{dt} + K(\psi_{n+1} + \psi_{n-1} - 2\psi_n) - (|\psi_n|^2 - 1)\psi_n = 0, \quad (42)$$

where we have made a simple change of variables, $\psi_n \to \psi_n \exp(-i\Psi_0^2 t)$, and introduced the parameter K defined in Eq. (28). Equation (42) may be viewed as a Hamiltonian model defined through the relation $i(d\psi_n/dt) = \delta H/\delta\psi_n^*$, where H is the system Hamiltonian [cf. Eq. (33)]

$$H = \sum_n \left\{ K|\psi_{n+1} - \psi_n|^2 + \frac{1}{2}(|\psi_n|^2 - 1)^2 \right\}. \quad (43)$$

If the solution ψ_n is a slowly varying function of n, one may expand $\psi_{n\pm1}$ into a Taylor series recovering the Hamiltonian of the continuous NLS equation.

Assuming the discreteness effects are small, we seek the approximate dark-profile mode of the discrete model (42) in the form

$$\psi_n(t) = B\tanh[B(na - x_0)] + iA, \quad (44)$$

where the parameters A and B are connected by the relation $A^2 + B^2 = 1$ following from the asymptotic behavior of the solution for $n \to \pm\infty$. The parameters $A(t)$ and $x_0(t)$ are taken as *collective variables*, x_0 is the soliton's coordinate, and A is connected with the phase jump across the soliton. Substituting Eq. (44) into Hamiltonian (43) and using, as above, the Poisson formula (see, e.g., Ref. [7] and Eqs. (38) and (39)], we calculate the effective Hamiltonian corresponding to the solution (44),

$$H = \frac{4}{3}B^3 + B^3\varepsilon_{PN}(aB)\cos\left(\frac{2\pi x_0}{a}\right), \quad (45)$$

where

$$\varepsilon_{PN}(x) = \int_{-\infty}^{+\infty} \frac{dz}{\cosh^4 z}\cos\left(\frac{2\pi z}{x}\right). \quad (46)$$

As a matter of fact, after introducing dimensionless variables, $2Ka^2 = 1$, we come to the results given by Eq. (38) and (39). However, the important difference between Eqs. (45), (46) and (38), (39) is that the parame-

ter B in (45), which is equal to $1/a\sqrt{2K}$ in Eq. (39), is treated now as a dynamical variable.

To obtain correctly the evolution equations corresponding to the Hamiltonian (45), we should define the corresponding conjugated variables, the generalized coordinate and momentum. If we choose x_0 as a generalized coordinate, it may be checked that the conjugated momentum P coincides with the renormalized field momentum of the continuous NLS equation calculated as (see details in Ref. [30])

$$P = \frac{i}{2}\int\left(u\frac{\partial u^*}{\partial x} - u^*\frac{\partial u}{\partial x}\right) - \arg u\Big|_{-\infty}^{+\infty}. \tag{47}$$

If we introduce the soliton phase angle θ through the relations $B = \cos\theta$ and $A = \sin\theta$, the momentum (47) takes the form [30]

$$P = -[\sin(2\theta) + 2\theta]. \tag{48}$$

The Hamiltonian equations of motion for the conjugated variables x_0 and P follow from the well-known relations

$$\frac{dx_0}{dt} = \{H, x_0\} = \frac{\partial H}{\partial P}, \quad \frac{dP}{dt} = \{H, P\} = -\frac{\partial H}{\partial x_0}, \tag{49}$$

where $\{x_0, P\} = 1$, and $\{\}$ stands for the Poisson brackets. In the limit of rather weak discreteness effects we may neglect the second (small) term in the equation for x_0 and finally obtain the system of equations

$$\frac{dx_0}{dt} \approx \sin\theta, \tag{50}$$

$$\frac{d\theta}{dt} = -\frac{\pi}{4a}\cos\theta\,\varepsilon_{PN}(a\cos\theta)\sin\left(\frac{2\pi x_0}{a}\right). \tag{51}$$

Equations (50), (51) immediately indicate that the A mode (i.e., that corresponding to $x_0 = 0$ when the soliton's center is located at a particle site) must be *stable*, whereas the B mode (i.e., that corresponding to $x_0 = a/2$ when the soliton's center is located between the neighboring particle sites) must be *unstable* [31]. The frequency of small-amplitude oscillations Ω_{PN}^2 around the point $x_0 = 0$ is given by the result,

$$\Omega_{PN}^2 = \frac{\pi^2}{2a^2}\varepsilon_{PN}(1/\sqrt{K}). \tag{52}$$

2. *High-frequency modes*

The collective-coordinate analysis presented above may be easily reproduced for the case of high-frequency dark-profile modes, when the dark soliton is excited on a modulationally stable background consisting of out-of-phase particles oscillations, and this is the case of $\lambda > 0$. Introducing the function φ_n through the relation

$$\psi_n = (-1)^n\varphi_n e^{i\omega_m t}, \tag{53}$$

where $\omega_m = 4D + \lambda\psi_0^2$, and the parameter K defined in Eq. (28), we come to the equation for the function φ_n,

$$i\frac{d\varphi_n}{dt} - K(\varphi_{n+1} + \varphi_{n-1} - 2\varphi_n) + (|\varphi_n|^2 - 1)\varphi_n = 0. \tag{54}$$

Equation (54) looks very similar to Eq. (42) and its dark-soliton solution has the form [cf. Eq. (44)]

$$\varphi_n(t) = B\tanh[B(na - x_0)] - iA, \tag{55}$$

where the parameters A and B are connected again by the relation $A^2 + B^2 = 1$, so that A and x_0 may be selected as two collective variables. As a result, the system Hamiltonian H and the field momentum P (which is used as a generalized variable) differ from Eqs. (45) and (48) just in the sign in front of both expressions, so that the stability properties resulting from the motion equations do not change: the A mode corresponding to $x_0 = 0$ is predicted to be stable, whereas the B mode ($x_0 = a/2$) is unstable.

The collective-coordinate analysis presented above is based on the simplest ansatz (44) or (55). In fact, such an ansatz fixes a relation between the pulse amplitude and width, restricting the quantity of independent variables. Such a restriction may affect the stability properties of the localized modes, so that we need to check these predictions by direct numerical simulations.

B. Numerical results

After analyzing the stationary configurations related to extrema of the effective PN potential and their stability, one may naturally ask how the PN potential affects the dark-soliton dynamics. Intuitively, it is clear that the main effect produced by an effective discreteness-induced inhomogeneity to the dark soliton [see, e.g., the result given by Eq. (45) for the soliton energy in the quasicontinuum approximation] is the pinning of the soliton at certain places in the lattice (corresponding to minima of the PN potential). Nevertheless, one should expect that if the soliton is able to overcome the PN barrier, it will start to move across the lattice. In the framework of this picture the B mode (which is predicted to be unstable) does not require any initial velocity for the soliton to start such a motion, whereas the threshold effect must be observed for the A mode, which in the collective-coordinate phenomenology corresponds to a minimum of the effective PN potential.

To check this qualitative picture we have analyzed the effect of lattice discreteness numerically starting from a slightly "excited" state corresponding to a dark soliton with a small initial velocity (i.e., small value of the parameter A). The latter simply means that, taking into account the results of the continuum limit approach given by Eq. (11), we start from the profile approximated by Eq. (44) but with $A \neq 0$ [see Eq. (11)]. As has been mentioned above, the parameter A defines the initial velocity of the dark soliton.

We always start at the middle of the chain consisting

of 101 particles, but with the soliton's coordinate x_0 selected in the region $0 \leq x_0 \leq a/2$. Figures 5(a) and 5(b) present the case of the B mode, i.e., that with the soliton's center selected just at the middle between the neighboring particle sites. As may be seen from Fig. 5(b), this stationary state is unstable in the sense mentioned above [31] because the minimum initial velocity ($A = 10^{-3}$ in Fig. 5) causes the soliton to move through the lattice. The same behavior is observed for the zero initial velocity but at x_0 slightly shifted from the equilibrium position, i.e., $x_0 = a/2 + \xi$, where $\xi \ll a$. We also checked the stability properties of the high-frequency B mode [with out-of-phase oscillations of the neighboring particles in the lattice, see Fig. 3(b)] and we observe exactly the same behavior as for the low-frequency in-phase dark solitons. Thus, the phenomenological picture based on the effective PN potential to the soliton's coordinate correctly predicts discreteness-induced instability of the B modes, i.e., those centered between the neighboring particle sites in the lattice.

A similar numerical investigation has been carried out for the A modes by using two types of initial conditions. In the first case, the soliton's center is fixed at the site $n = 50$ but its initial velocity A is varied. In the second case, the initial velocity is chosen to be zero but the soliton's position is varied in the interval $0 \leq x_0 \leq a/2$. The final pictures given by these two types of initial conditions are very similar, so that below we discuss the results corresponding to the initial conditions of the first type.

If the soliton's velocity is not zero and it is above a certain threshold value A_{cr} [i.e., $A_{cr} \approx 0.036$ at $K = 1.0$ or $A_{cr} \approx 0.06$ at $K = 0.8$], the soliton dynamics is likely the same as in the case of the unstable B mode. The soliton starts to move along the lattice; however, some (small) part of the energy is emitted as a transition radiation. This type of the soliton's dynamics is consistent with the physical picture given by the PN effective potential. As a matter of fact, for rather large values of its velocity the soliton may escape the potential well, and the threshold value of the soliton's velocity may be approximately estimated from the simple relation $\varepsilon_{PN} \approx E_{kin}$, where ε_{PN} is the PN barrier and E_{kin} is the kinetic energy of the effective particle in the collective-coordinate approach.

When the soliton's initial velocity is selected below the threshold value A_{cr}, we observe a very interesting phenomenon. During a certain time the dark soliton oscillates with the frequency close to the value defined by Eq.

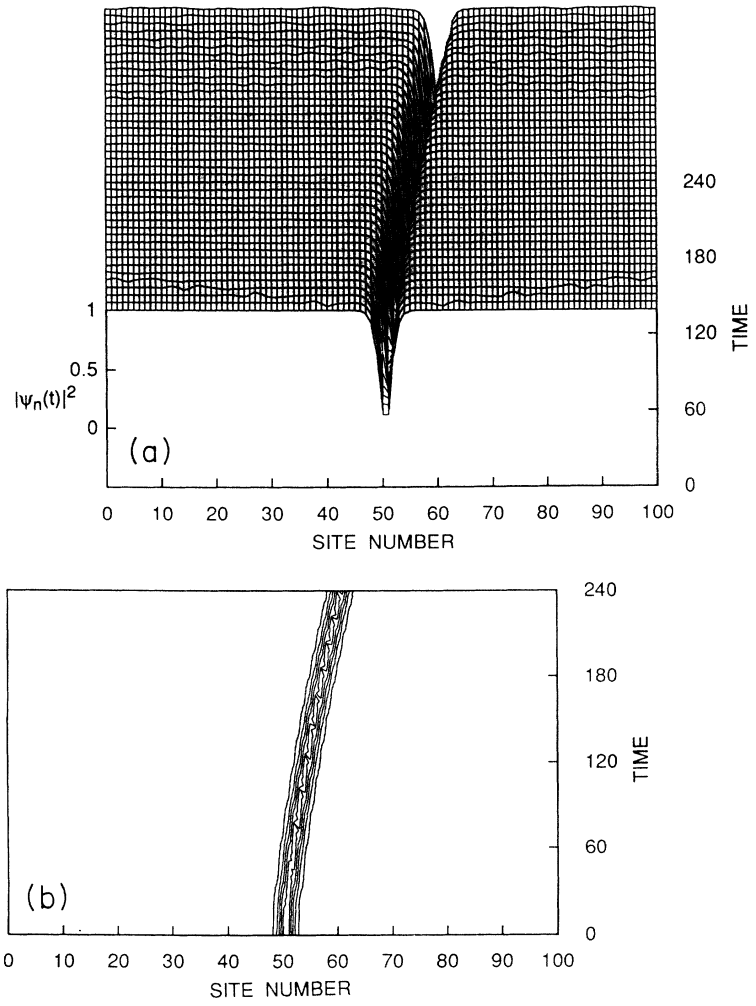

FIG. 5. Spatiotemporal dynamics of a dark soliton (a) and the corresponding contour plot (b) for the case when the soliton's center is selected between the neighboring particles sites, i.e., here between $n = 50$ and $n = 51$ (the B mode). This stationary state is obviously unstable because even the minimum value of the initial velocity, $A = 10^{-3}$, gives rise to the soliton motion.

(52), but *the amplitude of such oscillations gradually increases* so that, as soon as it reaches the value $a/2$, the soliton escapes from the potential well. Figures 6 and 7 display two types of the dark-soliton dynamics in the lattice when the initial soliton's velocity is selected below the threshold value. In the first case, shown in Figs. 6(a) and 6(b), after a series of oscillations the dark soliton escapes to the right, whereas in the second case, it escapes to the left. The difference in the resulting dynamics of the dark soliton is caused by different initial parameters selected for simulations. In fact, when we fix all other parameters and gradually increase only the one, either the initial soliton's velocity or the value of the relative soliton's position (in respect to the PN minimum), the propagation direction of the escaping soliton periodically changes. In Figs. 8 and 9 we present such an oscillating dependence measuring the relative position of the soliton center at $t_k = 600$ for $K = 1.0$ and at $t_k = 200$ for $K = 0.8$, respectively. The relative position is defined as the value $\Delta N = N - N(0)$, where N is the number of the particle site where the soliton minimum is situated at time t_k, and $N(0) = 50$. Only several points presenting such oscillating dependencies are shown in Figs. 8 and 9 (especially in Fig. 9, where the solid line is defined just to guide the eye), but the transitions between the soliton's escapes to the right and to the left are very sharp, and there are no points lying on the line $\Delta N = 0$, i.e., *we do not observe trapped states of a dark soliton in the lattice.* Thus, unlike the prediction which follows from the simple collective-coordinate analysis, the dark-profile soliton in the lattice seems always unstable.

It seems to us such an instability (which has no analog in the theory of spatially localized modes in lattices) originates from an interplay between the soliton's width and amplitude. In the continuum case these two parameters are connected by a simple relation and a change in one of them causes a change in the other. In a discrete lattice, when the coupling between particles is rather weak, dark solitons may exist being localized only on a few particles, so that the soliton's width is not strongly connected to the soliton's amplitude. When we start from an approximate solution originated from the continuous approximation, the dark-profile mode tries to adjust the width and amplitude of the solution to create a mode close to an exact solution of the lattice equation. Such an adjustment causes periodic oscillations of the effective PN barrier. As a matter of fact, the similar effect must be observed for bright solitons as well, but in the case of dark solitons

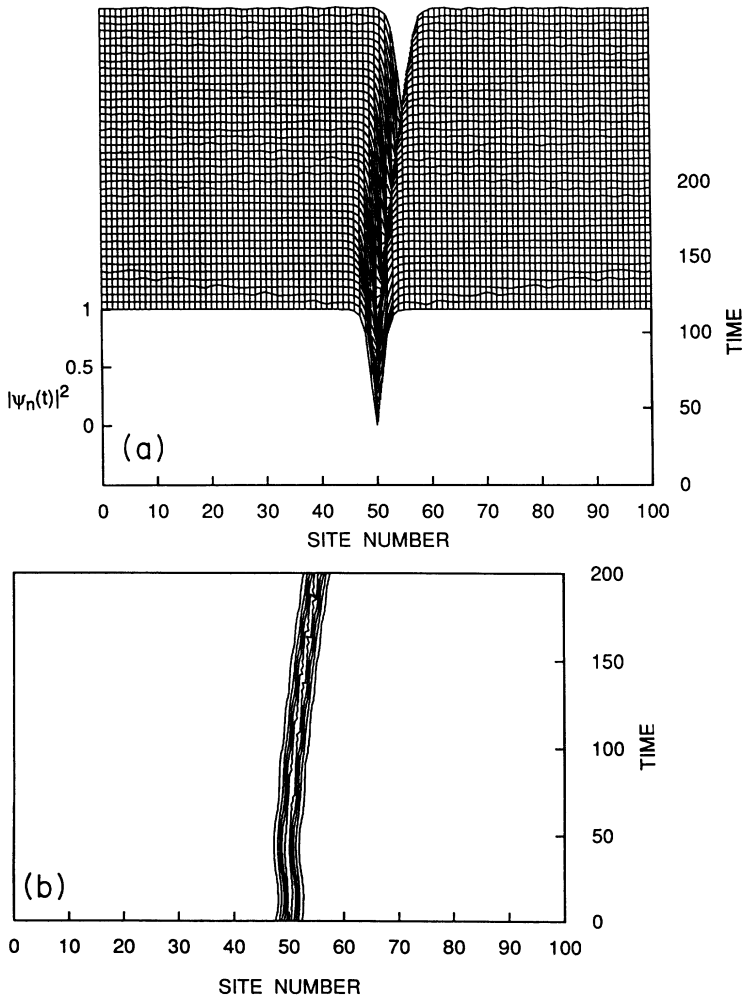

FIG. 6. The same as in Figs. 5(a) and 5(b) but for the soliton's center selected at $n = 50$ (the A mode). The initial velocity is $A = 0.02$. As clearly seen from the contour plot (b), after a few oscillations the dark soliton escapes from the potential well and it starts to move to the right.

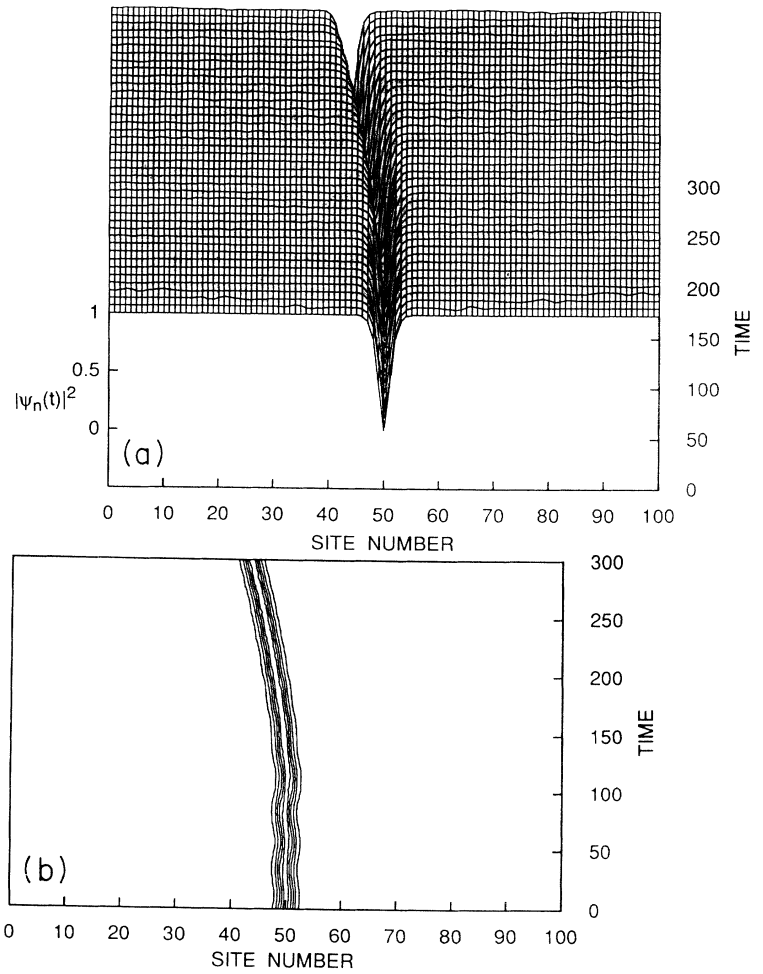

FIG. 7. The same as in Figs. 6(a) and 6(b) but for $A = 0.01$. In this case many more oscillations are observed and finally the dark soliton escapes to the left.

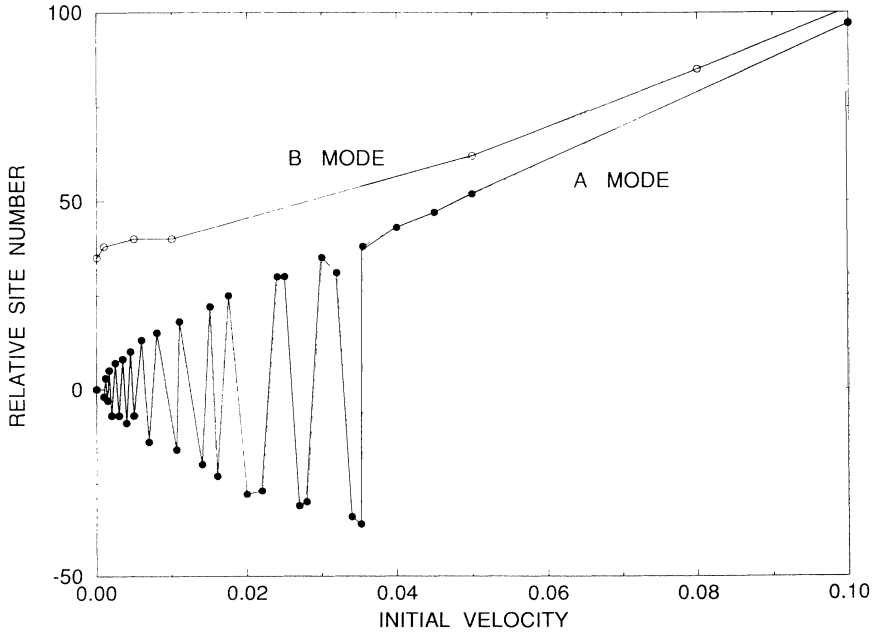

FIG. 8. The resulting picture of the dark-soliton instabilities at $K = 1.0$ presented as the relative position of the soliton at $t_k = 600$ vs the soliton's initial velocity. The curve shown by open circles corresponds to the B mode; there is no threshold for this mode to move. The oscillating dependence corresponds to the B mode. Above the threshold value of the soliton's velocity the soliton dynamics is similar to that for the A mode, i.e., the soliton always moves to the direction selected by the initial conditions. However, below the threshold velocity the soliton may escape to the right or to the left, depending on values of either the initial soliton velocity or position.

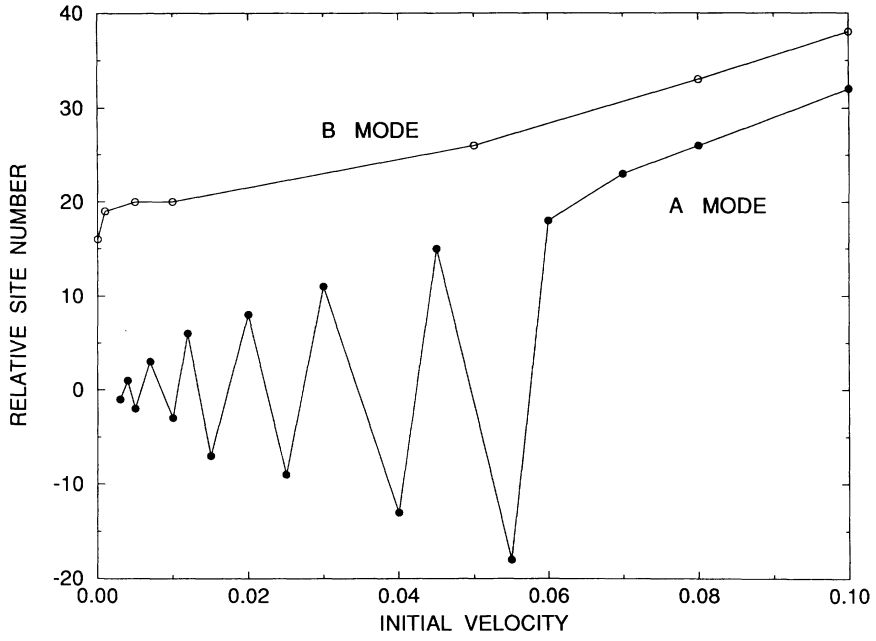

FIG. 9. The same as in Fig. 8, but at $K = 0.8$ at $t_k = 200$.

any change of the soliton's amplitude immediately causes a corresponding change in the soliton's velocity, and this effect is absent for the bright solitons which in the quasi-continuous limit have the amplitude and velocity as two independent parameters. Therefore, oscillations of the shape of the effective PN potential cause growing oscillations of the soliton itself similar to the effect of parametric resonance, and finally this helps the soliton to escape from the potential well. As a result, even being at a bottom of the effective PN potential, the dark soliton is dynamically unstable and this instability seems to be caused solely by discreteness effects.

V. CONCLUSIONS

In conclusion, we have analyzed effects of discreteness on dark-profile localized modes in the lattice NLS equation that arises naturally when one studies the analog of envelope solitons in models of solids describing dynamics of a chain of particles on a substrate (on-site) nonlinear potential. In the case of small-amplitude dark solitons, when the width of the soliton is much larger than the lattice spacing, the lattice discreteness may drastically modify the dispersion properties of waves and this effect, as has been shown in the present paper, may give birth to antidark solitons which propagate as bright solitons on a modulationally stable background. Such solitons may be analyzed in the framework of an effective Korteweg–de Vries equation by means of asymptotic methods.

In the case when the soliton's width is not very large, the effects produced by discreteness to the dark soliton may be understood as arising from an effective periodic potential similar to the well-known PN potential for topological kinks in the Frenkel-Kantorova model. This PN potential may affect the mobility of a dark soliton in the sense that one should overcome a certain energy barrier, the PN barrier, to get a dark soliton propagating relatively to the background. We have calculated the PN barrier numerically and analytically, using in the latter case a strong-coupling approximation and applying a Poisson formula. However, numerical simulations display additional instabilities of the dark soliton. Even being at the bottom of a PN potential well, the initially excited dark soliton starts to move to the right or to the left after a series of periodic oscillations with growing amplitude. An intuitive picture for such discreteness-induced instabilities has been presented, and the novelty of these instabilities for the discrete soliton bearing models has been emphasized.

ACKNOWLEDGMENTS

The work of Yu. K. was partially supported by the Australian Photonics Cooperative Research Centre (APCRC). He is also indebted to Nikos Flytzanis for stimulating discussions.

[1] M. Peyrard and M.D. Kruskal, Physica D **14**, 88 (1984).
[2] N. Flytzanis, St. Pnevmatikos, and M. Remoissenet, J. Phys. C **18**, 4603 (1985).
[3] A.J. Sievers and S. Takeno, Phys. Rev. Lett. **61**, 970 (1988).
[4] R. Boesch and M. Peyrard, Phys. Rev. B **43**, 8491 (1991).
[5] Yu.S. Kivshar and M. Peyrard, Phys. Rev. A **46**, 3198 (1992).

[6] Yu. S. Kivshar and D. K. Campbell, Phys. Rev. E **48**, 3077 (1993).
[7] Ch. Claude, Yu.S. Kivshar, O. Kluth, and K.H. Spatschek, Phys. Rev. B **47**, 14 228 (1993).
[8] O.A. Chubykalo, A.S. Kovalev, and O.V. Usatenko, Phys. Lett. A **178**, 129 (1993).
[9] Yu.S. Kivshar, Phys. Rev. Lett. **70**, 3055 (1993).
[10] T. Dauxois and M. Peyrard, Phys. Rev. Lett. **70**, 3935 (1993).
[11] D.B. Duncan, J.C. Eilbeck, H. Feddersen, and J. A. D. Watties, Physica D **68**, 1 (1993).
[12] D. Cai, A.R. Bishop, and N. Grønbech-Jensen, Phys. Rev. Lett. **72**, 591 (1994).
[13] D.N. Christodoulides and R.I. Joseph, Opt. Lett. **13**, 794 (1988).
[14] Yu.S. Kivshar, Opt. Lett. **18**, 1147 (1993).
[15] R.F. Peierls, Proc. R. Soc. London **52**, 34 (1940); F.R.N. Nabarro, *ibid.* **59**, 256 (1947); for more discussion see, e.g., F.R.N. Nabarro *Theory of Crystal Dislocations* (Dover, New York, 1987), and for detailed calculational examples, see, e.g., R. Hobart, Phys. Rev. **36**, 1948 (1965).
[16] K. Yoshimura and S. Watanabe, J. Phys. Soc. Jpn. **60**, 82 (1991).
[17] B. Luther-Davies and Yang Xiaoping, Opt. Lett. **17**, 496 (1992); Yang Xiaoping, B. Luther-Davies, and W. Królikowski, Int. J. Nonlin. Opt. Phys. **2**, 1 (1993).
[18] Yang Xiaoping, Yu.S. Kivshar, B. Luther-Davies, and D.B. Andersen, Opt. Lett. **19**, 344 (1994).
[19] Yu.S. Kivshar, IEEE J. Quantum Electron. **28**, 250 (1993).
[20] W. Królikowski, U. Trutschel, C. Shmidt-Hattenberger, and M. Cronin-Golomb, Opt. Lett. **19**, 320 (1994).
[21] A.B. Aceves, C. De Angelis, S. Trillo, and S. Wabnitz, Opt. Lett. **19**, 332 (1994).
[22] W. Królikowski and Yu.S. Kivshar (unpublished).
[23] J.C. Eilbeck, P.S. Lomdahl, and A.C. Scott, Physica D **16**, 318 (1985).
[24] H. Willairne, O. Cardoso, and P. Tabeling, Phys. Rev. Lett. **67**, 3247 (1991).
[25] Yu.S. Kivshar, Phys. Lett. A **173**, 172 (1993).
[26] Yu.S. Kivshar, Phys. Rev. A **42**, 1757 (1990); **43**, 1677 (1991).
[27] Yu.S. Kivshar and V.V. Afanasjev, Phys. Rev. A **44**, R1446 (1991).
[28] O.A. Chubykalo, V.V. Konotop, and L. Vázquez, Phys. Rev. B **47**, 7971 (1993).
[29] Yu.S. Kivshar and B. A. Malomed, Rev. Mod. Phys. **61**, 763 (1989).
[30] Yu.S. Kivshar and X. Yang, Phys. Rev. E **49**, 1657 (1994).
[31] We should emphasize here that in Secs. III and IV of this paper we use the terms "instability" and "unstable state" in a different sense than that in which they are usually used in general for different problems of nonlinear dynamics. As a matter of fact, *instability* here does not mean that a dark soliton decays. Instead, this means that the stationary state where the soliton is at rest is unstable and it starts to move (but a movement does not mean instability in general). This kind of instability of stationary states is usually considered in the context of nonlinear optics [see, e.g., D.J. Mitchell and A.W. Snyder, J. Opt. Soc. Am. B **10**, 1572 (1993) and references therein].